Univerzita Karlova v Praze

1. lékařská fakulta

Autoreferát disertační práce

The Role of Uncoupling in Down-regulation of Reactive Oxygen Species

RNDr. Jan Ježek

Praha 2009

Doktorské studijní programy v biomedicíně

Univerzita Karlova v Praze
a Akademie věd České republiky

Obor: Biochemie a patobiochemie

Předseda oborové rady: Prof. MUDr. Jiří Kraml, DrSc.

Školicí pracoviště: Fyziologický ústav AV ČR
Oddělení 75, Biofyziky
membránového transportu

Autor: RNDr. Jan Ježek

Školitel: RNDr. Markéta Žáčková, Ph.D.

Školitel konsultant: RNDr. Petr Ježek, DrSc.

Oponenti:

……..
……..
……..

Autoreferát byl rozeslán dne: .....

Obhajoba se koná dne: ……..... v ……... hod.
kde ……...
……...

S disertací je možno se seznámit na děkanátě
1. lékařské fakulty Univerzity Karlovy v Praze

ABBREVIATIONS

Amplex Red	N-acetyl-3,7-dihydroxyphenoxazine
ATP	adenosine 5'-triphosphate
BCECF, AM	2',7'-bis-(2-carboxyethyl)-5-(and-6)-carboxy-fluorescein, acetoxymethyl ester
BEL	bromoenol lactone
BSA	bovine serum albumin
Ctrl	control
DecylTPP	decyltriphenylphosphonium bromide
EIPA	5-(N-ethyl-N-isopropyl)amiloride
FCCP	carbonyl cyanide 4-(trifluoromethoxy)phenyl-hydrazone
GDP	guanosine 5'-diphosphate
GLC5	5 mM glucose-cultivated HepG2 cells
GLC25	25 mM glucose-cultivated HepG2 cells
GM	glutamate plus malate
GTP	guanosine 5'-triphosphate
HepG2	human hepatocellular carcinoma cells
HRP	horseradish peroxidase
$iPLA_2$	calcium-independent phospholipase A_2
Lac	lactate
$MitoQ_{10}$	10-(6'-ubiquinonyl)decyltriphenylphosphonium methanesulfonate
mtDNA	mitochondrial DNA
$mtPLA_2$	mitochondrial phospholipase A_2

OXPHOS	galactose/glutamine-cultivated HepG2 cells
PLA_2	phospholipase A_2
Q-pool	quinone pool
Q-site	quinone-binding site
ROS	reactive oxygen species
Rot	rotenone
SkQ1	10-(6'-plastoquinonyl)decyltriphenyl-phosphonium
Succ	succinate
TBHP	*tert*-butyl hydroperoxide
TTFA	2-thenoyltrifluoroacetone
UCP	uncoupling protein
UCP2-KO	UCP2 knockout mice
UCP2-WT	UCP2 wild-type mice

Remainder of ROS and RNS nomenclature

FAOOH	fatty acid hydroperoxide
H_2O_2	hydrogen peroxide
$O_2^{\bullet-}$	superoxide
PLOOH	phospholipid hydroperoxide

Notation for biophysical quantities

Δp	proton motive force

CONTENTS

1 SOUHRN

Produkci superoxidu komplexem I lze tlumit odpřažením, které urychlí elektronový tok a protonové pumpování komplexu I. Za podmínek, kdy je znemožněné protonové pumpování komplexu I, např. v důsledku mutací mitochondriální DNA kódující podjednotku ND2, ND4 nebo ND5 komplexu I, podílející se na protonovém pumpování, by terapeutická intervence založená pouze na odpřažení nebyla účinná. V pokusech je model poruchy protonového pumpování simulován hydrofobním amiloridem EIPA. My jsme poprvé ukázali, že EIPA je inhibitor protonového pumpování i pro mitochondriální komplex I. Hledali jsme agens, jenž by na rozdíl od opřažení tlumilo oxidační stres v důsledku omezeného protonového pumpování komplexu I. Ubichinon cílený do mitochondrií $MitoQ_{10}$ se pro tento účel ukázal být účinným antioxidantem při zvýšené produkci superoxidu způsobené zpomaleným elektronovým tokem na komplexu I. V souvislosti s prooxidačními účinky $MitoQ_{10}$ je nutné jej při léčbě cílit do místa poškozené tkáně. Aktivací mitochondriální fosfolipasy $iPLA_2$ mírným oxidačním stresem jsou uvolňovány hydroperoxidy mastných kyselin sloužící jako cyklující substráty pro UCP2, jenž mírným odpřažením zpětnovazebně tlumí produkci reaktivních sloučenín kyslíku. Buňky s nižším zastoupením oxidativní fosforylace adaptují méně účinně na podmínky fyziologické normoxie. Glykolytické normoglykemické buňky adaptují na 5% kyslík zvýšením respirace ve stavu 4.

2 SUMMARY

Uncoupling attenuates Complex I-derived superoxide production by accelerating electron flux and proton pumping within Complex I. However, under circumstances leading to hampered proton pumping pathway within Complex I, *e.g.* due to aberrant mutations of mtDNA encoding either ND2, ND4 or ND5 Complex I H^+-pumping subunit, therapeutic strategy based simply on uncoupling would fail. Experimentally, hydrophobic amiloride EIPA mimicks the model of disabled H^+-pumping. We show for the first time that EIPA is a real inhibitor of H^+-pumping of mitochondrial Complex I. We searched for an agent that, unlike uncoupling, would be able to counteract oxidative stress associated with obstructed proton pumping of Complex I. Mitochondria-targeted ubiquinone $MitoQ_{10}$ proved to be an effective antioxidant for this purpose when the rate of superoxide formation was high due to the electron flow retardation within Complex I. Because of its pro-oxidant properties, targeted delivery of $MitoQ_{10}$ as a cure to the pathological tissue is necessary. Activation of mitochondrial phospholipase $iPLA_2$ by mild oxidative stress can provide free fatty acid hydroperoxides as the cycling substrates for UCP2 that initiates mild uncoupling leading to the attenuation of reactive oxygen species (ROS) production, as a part of feedback regulatory loop of lipid peroxidation. Cells with lower oxidative phosphorylation content adapt less efficiently to the conditions of physiological normoxia. Glycolytic normoglycemic cells adapt to 5% oxygen by elevated state 4 respiration.

3 INTRODUCTION

Mitochondria are essential organelles for eukaryotic aerobic metabolism, involving respiratory chain, citric acid cycle and β-oxidation pathways. The principal function of mitochondria is to generate energy by coupling respiration to the synthesis of ATP during a process called oxidative phosphorylation, but they are also involved in homeostasis of ROS, oxygen sensing, and other processes. Mitochondria play a central role in molecular physiology of the cell and their dysfunction is implicated in numerous pathophysiological states: cancer, diabetes mellitus II, cystic fibrosis, inflammation, cardiovascular and neurodegenerative diseases.

Reactive oxygen species evolve as a by-product of oxidative metabolism, and mitochondria represent the major source of ROS for the cell. Oxidative stress arises from surplus production of reactive oxygen species above the levels which are required for normal ROS homeostasis and signaling. ROS readily attack ambient biomolecules including DNA, proteins, and lipids. In healthy cells, excessive harmful ROS are decomposed by protective antioxidant systems.

The significance of mitochondrial uncoupling proteins (UCPs) lies in their ability to affect energetic status of mitochondria and to attenuate mitochondrial production of ROS. Fatty acid hydroperoxides may be the key elements of ROS-sensing signal pathways, acting as cycling substrates of uncoupling proteins during the feedback inhibition of lipoperoxidation.

4 OBJECTIVES AND HYPOTHESES

The purpose of this work was to study the relationship between the mechanisms of reactive oxygen species homeostasis and uncoupling in the context of mitochondrially related physiology and pathology [1]. The thesis encompasses four different selected aims in order to elucidate:

1) The Inhibition of Mitochondrial Complex I Proton Pumping

Superoxide production within mitochondrial Complex I is regulated by feedback pressure of the proton motive force (Δp) [2], that also limits H^+-pumping within the membrane arm of Complex I toghether with the accompanying conformational changes, which would retard the redox traffic at the peripheral arm of Complex I leading to prolonged half-lifes of ubisemiquinone species, hence giving rise to elevated $O_2^{\bullet -}$ production. In experiments, 5-(N-ethyl-N-isopropyl)amiloride (EIPA) substitutes for the block imposed by Δp.

2) The Mechanism of Action of Mitochondrial Matrix-targeted Ubiquinone $MitoQ_{10}$

Antioxidant role of $MitoQ_{10}$ can take place only when its reduced form $MitoQ_{10}H_2$ is regenerated by the participation of Complex II. $MitoQ_{10}$ accepts electrons from Complex I prior the downstream Q-site

blocked by rotenone [3]. Electron flow is further conveyed via a fraction of Complex II molecules operating in the reverse mode. The biased electron flow is then merged with the usual succinate-driven forward electron transfer pathway delivering electrons into the Q-pool.

3) Mitochondrial Phospholipase $iPLA_2$-Dependent Regulation of Uncoupling Protein UCP2

Oxidative stress-initiated lipid peroxidation gives rise to phospholipid hydroperoxides (PLOOHs). PLOOHs may serve as substrates for the mitochondrial Ca^{2+}-insensitive isoform of PLA_2, $iPLA_2$, releasing fatty acid hydroperoxides (FAOOHs). In turn, FAOOHs have the ability to act as cycling substrates for UCP2-mediated uncoupling [4]. Mild uncoupling would represent the last step of a hypothetical feedback regulatory loop leading to the direct attenuation of oxidative stress.

4) The Elevation of State 4 Respiration upon Adaptation to Physiological Normoxia

Adaptation of hepatocellular carcinoma HepG2 cells to 5% oxygen for the period of three days is similar to adaptation occurring during transfer from physiological normoxia to hypoxia *in vivo* [5].

5 MATERIALS AND METHODS

1) Isolation of Intact Mitochondria by Differential Centrifugation
   a) Isolation of Rat Liver Mitochondria
   b) Isolation of Mitochondria from HepG2 Cells
   c) Isolation of Rat Lung Mitochondria
   d) Isolation of Mouse Lung Mitochondria
2) Assay for Mitochondrial H_2O_2 Generation *In Vitro*

In vitro mitochondrial H_2O_2 production was assyed by using fluorescent monitoring of oxidation of Amplex Red by HRP [2, 6].

3) Assay for Polarographic Detection of Oxygen Consumption
   a) High-Resolution Respiration Measurements
   b) Respiration Measurements of Cells at Physiological O_2 Levels
4) Assay for Complex I Proton Pumping

H^+-pumping was evaluated as matrix alkalization indicated by BCECF fluorescence [7].

5) Cell Cultures
6) Statistical Analysis

Individual means were compared using Student's *t*-test with $P \leq 0.05$ considered to represent significantly different values from the control

(marked with an asterisk).

6 RESULTS

6.1 The Inhibition of Mitochondrial Complex I Proton Pumping

Proton pumping has been measured in BCECF, AM-loaded isolated rat liver mitochondria as a pH-sensitive fluorescence of BCECF, with mitochondrial matrix alkalinization reflecting the increase in H^+-pumping activity.

Matrix alkalinization was apparent after the addition of Complex I respiratory substrates 5 mM glutamate and 1 mM malate (Fig. 1*a*, *page 9*), and abolished after the addition of Complex III inhibitor stigmatellin (Fig. 1*a*, *page 9*), Complex I inhibitor rotenone, and a chemical uncoupler FCCP (not shown).

EIPA inhibits Complex I H^+-pumping in isolated rat liver mitochondria respiring in sate 4, which is reflected by the abolition of matrix alkalinization stimulated by EIPA added before glutamate and malate (Fig. 1*b*, *page 9*) or after the substrates, and even in the presence of monensin simulating Na^+/H^+ antiporter activity (not shown). The half-maximum effect for EIPA inhibition before the addition of glutamate and malate occurred at 27 μM EIPA (Fig. 2, *page 10*). EIPA inhibits Complex I H^+-pumping in isolated rat liver mitochondria respiring in sate 3 with the IC_{50} of 50 μM (Fig. 2, *page 10*). EIPA exerts no significant effects on respiration of isolated rat liver mitochondria (Fig. 2, *page 10*).

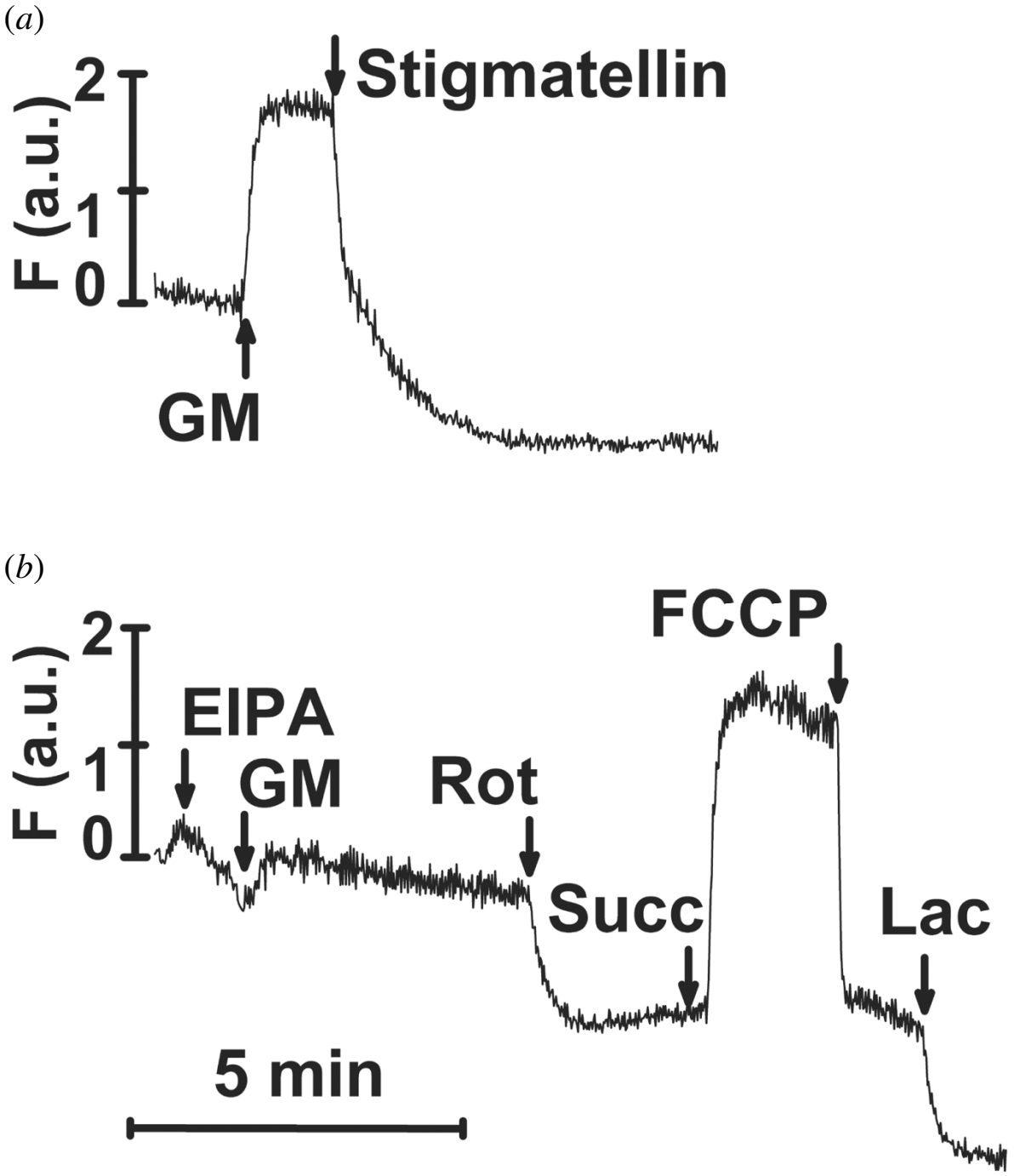

FIGURE 1 Glutamate and malate-driven H^+-pumping is prevented by EIPA in isolated rat liver mitochondria respiring in state 4. Matrix alkalinization is shown for the following additions: 5 mM glutamate plus 1 mM malate to both traces, and **(*a*)** 0.5 μM stigmatellin;

(***b***) 100 μM EIPA, 10 μM rotenone (Rot), 5 mM succinate (Succ), 1 μM FCCP, and 1 mM lactate (Lac).

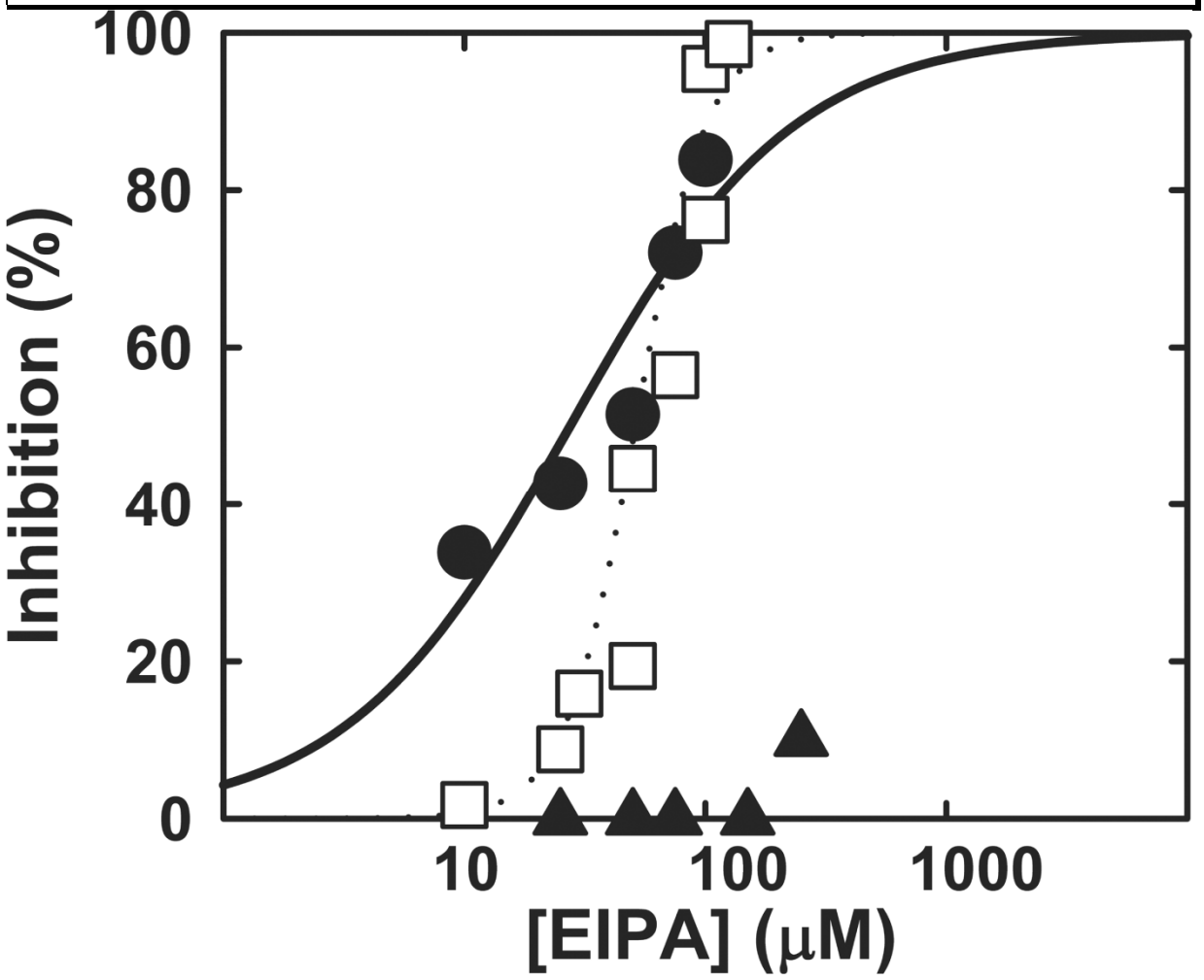

FIGURE 2 EIPA Dose-response curves for respiratory and H^+-pumping inhibition of isolated rat liver mitochondria. Inhibitory effects of EIPA were quantified for ● *closed circles*: H^+-pumping in state 4 as the decrease in matrix akalinization stimulated by glutamate and malate after the addition of EIPA, IC_{50} = 27 μM; □ *open squares*: H^+-pumping in state 3 as the acidification induced by EIPA after the addition of glutamate and malate, IC_{50} = 50 μM; ▲ *closed triangles*: respiratory rate in state 4.

6.2 The Mechanism of Action of Mitochondrial Matrix-targeted Ubiquinone $MitoQ_{10}$

The influences of $MitoQ_{10}$ on respiration of HepG2 cells were investigated by using high-resolution respirometry under two different cellular metabolic conditions. When cultivated in high glucose (25 mM), cells (GLC25) are forced to use glycolysis as the main metabolic pathway for energy production. $MitoQ_{10}$ accelerated state 3 respiration of GLC25 cells (Fig. 3, *page 12*), *i.e.* basal respiration before the addition of oligomycin, on average up to 1.5-fold over the initial value. The half-maximum activation took place on average at 0.8 nM $MitoQ_{10}$.

Analogous acceleration with comparable AC_{50} was obtained for HepG2 cells grown in medium containing galactose and glutamine (not shown). These cells rely predominantly on oxidative phosphorylation (OXPHOS cells) as the primary energy source.

At saturating doses of rotenone (20 μM), respiration of GLC25 and OXPHOS cells was suppressed down to residual 15% (Fig. 4, *page 13*), and 11% (not shown), respectively. Consequent pulses of $MitoQ_{10}$ reestablished 67% and 45% levels of state 3 respiration in GLC25 (Fig. 4, *page 13*) and OXPHOS cells (not shown), respectively. Respiration increase induced by $MitoQ_{10}$ requires Complexes II and III as judged from the sensitivity to TTFA and antimycin A, respectively (not shown). DecylTPP, which lacks the ubiquinone moiety, elicited an insignificant effect in cells but not in mitochondria isolated from rat liver or GLC25 cells (not shown).

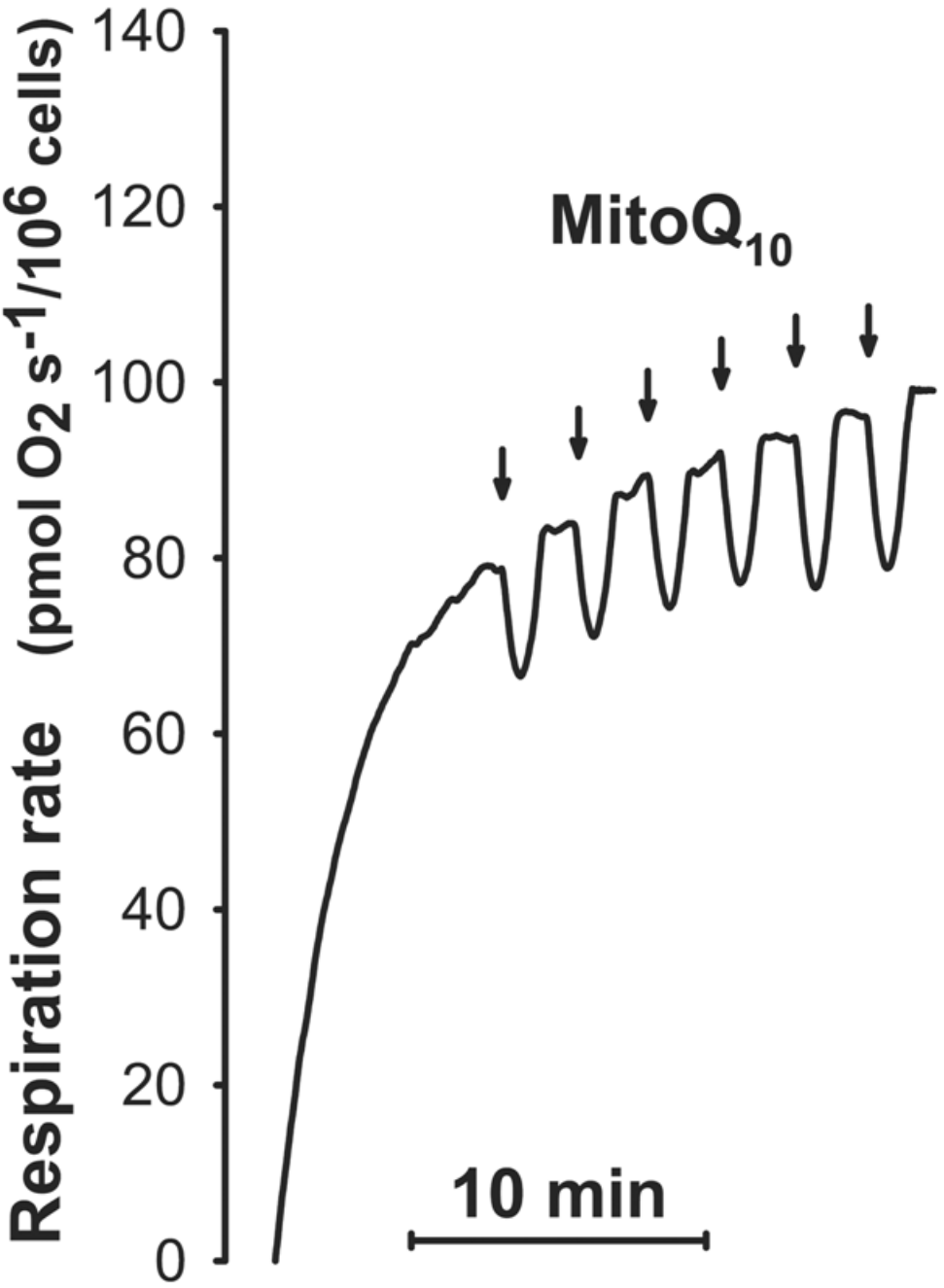

FIGURE 3 $MitoQ_{10}$ stimulates state 3 respiration of GLC25 HepG2 cells. Cells were treated, as indicated at each arrow, with 0.2 nM $MitoQ_{10}$.

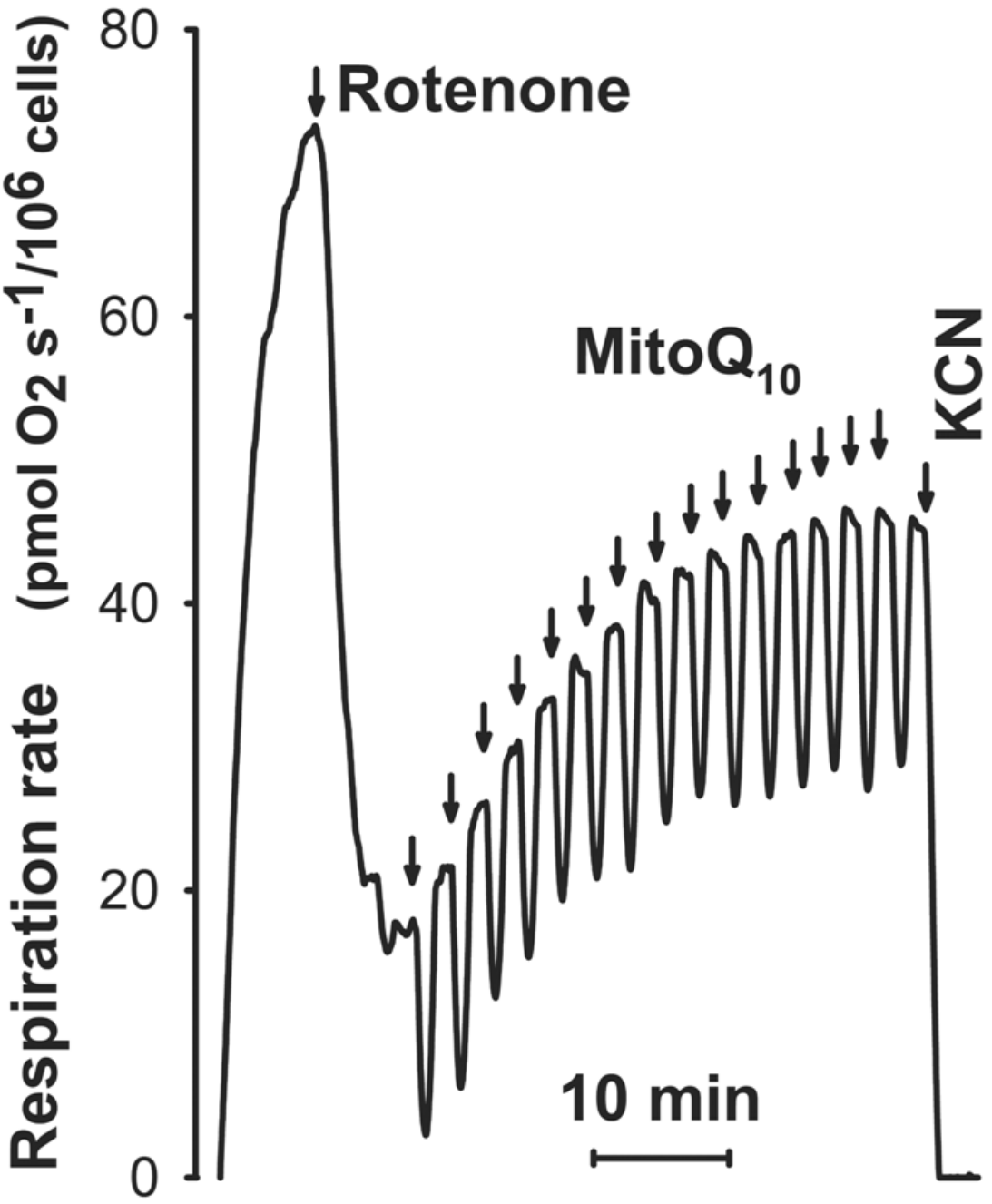

FIGURE 4 $MitoQ_{10}$ activation of state 3 respiration in the presence of rotenone. GLC25 cells were treated, as indicated at each arrow, with 1 μM rotenone, 0.2 nM $MitoQ_{10}$ and 1 mM KCN.

6.3 Mitochondrial Phospholipase $iPLA_2$-Dependent Regulation of Uncoupling Protein 2

High-resolution respirometry was used to monitor respiration of isolated rat lung mitochondria respiring in state 4 with succinate as a substrate. Pro-oxidant *tert*-butyl hydroperoxide (TBHP) treatment was used to simulate lipid peroxidation. It was shown before that phospholipases A_2 are activated upon TBHP treatment [8]. The resulting lipoperoxidized mitochondria would serve as the model for fatty acid release from membrane phospholipids.

Tert-butyl hydroperoxide (5 μM) induces increase in respiration of rat lung mitochondria (Fig. 5, *page 15*), which reflects more pronounced uncoupling.

Mitochondrial $iPLA_2$ promotes uncoupling that is UCP2-dependent, because the respiration increase induced by TBHP was absent in UCP2-KO mice (Fig. 5, *page 15*) and fully inhibited by BSA, which removes free fatty acids, bromoenol lactone (BEL), a specific inhibitor of phospholipase $iPLA_2$ isoforms β and γ [9], and partially inhibited by GTP (not shown) and GDP (Fig. 5, *page 15*), inhibitors of UCP2 [10].

H_2O_2 production monitored with Amplex Red during TBHP-induced oxidative stress and its acceleration by BEL and BSA (Fig. 6, *page 16*) indicates that with the removal of free FAOOHs by BSA or with the blockage of their cleavage off the phospholipids by BEL the UCP2-dependent attenuation of TBHP-stimulated mitochondrial $O_2^{\bullet -}$ production is not observed.

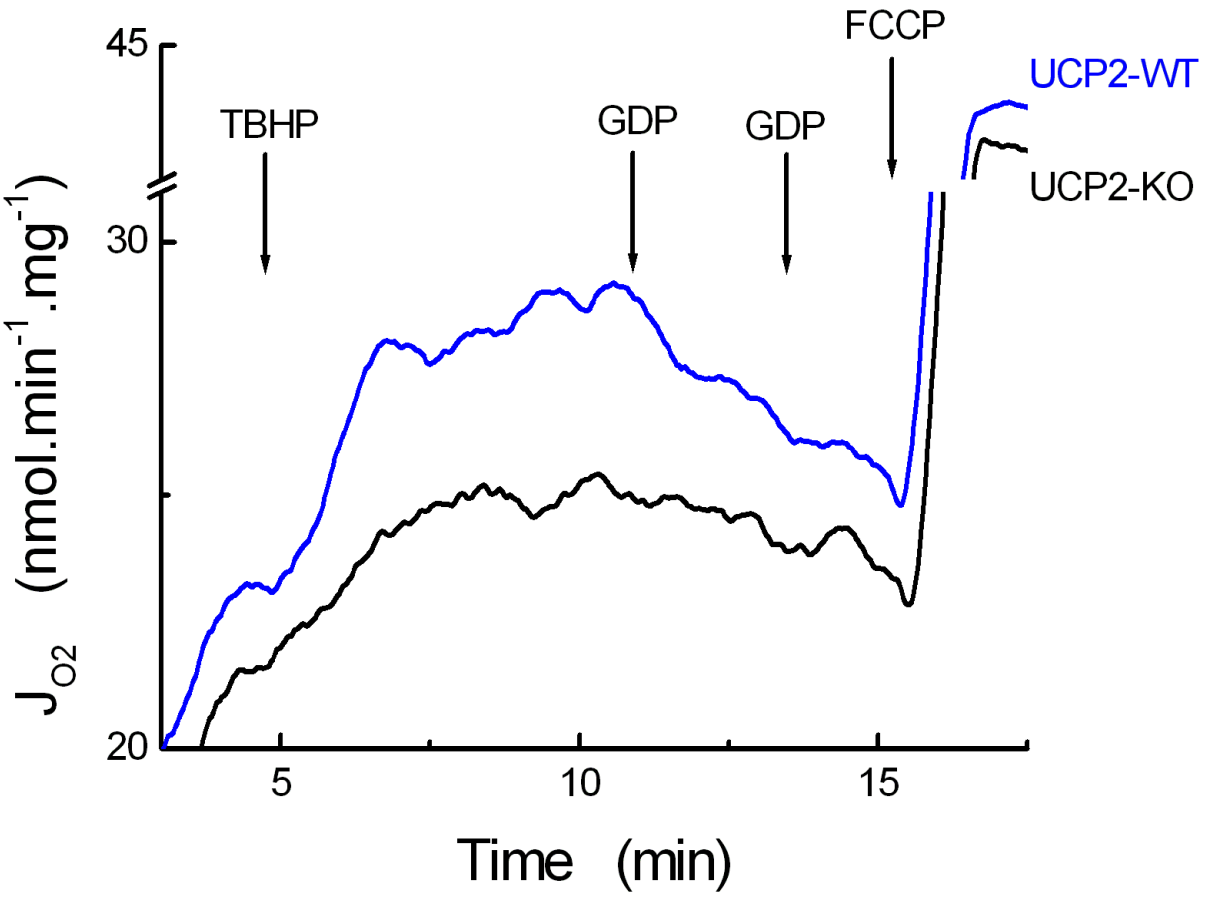

FIGURE 5 The effect of TBHP and GDP on lung mitochondria isolated from UCP2-WT and UCP2-KO mice. Mitochondria (0.1 mg/ml) were allowed to respire in the assay medium containing 10 mM succinate, 1 μM rotenone, and 1 μg/ml oligomycin. Rates are shown for the following additions: 25 μM TBHP, 0.5 mM GDP (added twice), and 20 nM FCCP to both traces. Mitochondria were isolated from *black trace*: UCP2-KO mice; *blue trace*: UCP2-WT mice. Y-axis was manipulated to include the off-scale part of both traces.

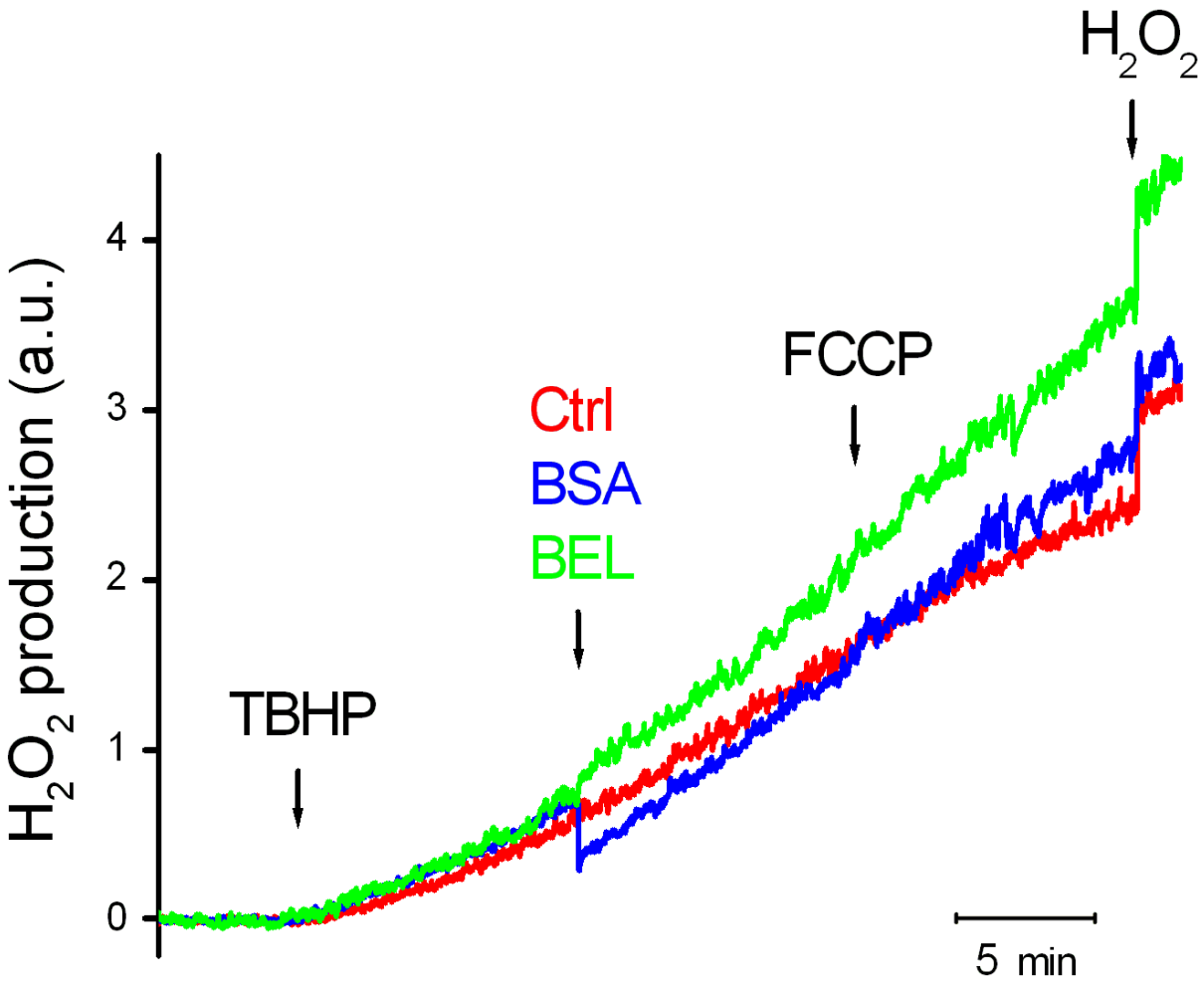

FIGURE 6 TBHP-induced generation of H_2O_2 and appearance of ROS by isolated rat lung mitochondria is accelerated by BSA and bromoenol lactone. Mitochondria (0.2 mg/ml) were allowed to respire in the assay medium containing 10 mM succinate, 1 μM rotenone, and 1 μg/ml oligomycin. Rates are shown for the following additions: 10 μM TBHP, 50 nM FCCP, and 0.1 μM H_2O_2 to all traces, and *red trace*: no additions (Ctrl); *blue trace*: 0.2 mg/ml BSA; *green trace*: 10 μM BEL.

6.4 The Elevation of State 4 Respiration upon Adaptation to Physiological Normoxia

HepG2 cells were incubated at 5% O_2 for three days under three different metabolic states. The metabolic status of the cell was modulated by varying cell culture medium components with OXPHOS cells (cultivated in galactose plus glutamine) utilizing mainly oxidative phosphorylation, and GLC5 or GLC25 cells (cultivated in 5 mM or 25 mM glucose, respectively) relying predominantly on anaerobic pathways of energy production, as previously established [2, 6]. After three days, respiratory properties of cells incubated either at atmospheric (21%) oxygen or at 5% O_2 were assessed either at atmospheric or 5% O_2 levels. Normal condition refers to the atmospheric cultivation of cells and respiration measurement initiated at atmospheric O_2. Adapted condition refers to a three-day cultivation of cells at 5% O_2 and respiration measurement initiated at 5% O_2. Instant adapted condition means atmospheric cultivation and the cells measured at initial 5% O_2. Recovered condition means three-day cultivation at 5% O_2 and the cells measured at initial atmospheric O_2.

Glycolytic cells are more prone to decline of respiration after a 3-day adaptation to 5% O_2 (Fig. 7, *page 18*), whereas OXPHOS cells utilize more efficient oxidative phosphorylation, as seen from their elevated state 3/state 4 respiratory control ratio (Fig. 8, *page 19*). Glycolytic normoglycemic cells adapt to 5% oxygen by elevated state 4 respiration, which can be judged from the decrease of state 3/state 4 respiratory

control ratio (*i.e.* the ratio of respiratory rates before and after the addition of oligomycin, Fig. 8, *page 19*) and the decrease of uncoupled state/state 4 respiratory control ratio (the ratio of respiratory rates after and before the titration of FCCP to saturation, not shown) after a 3-day adaptation to 5% O_2.

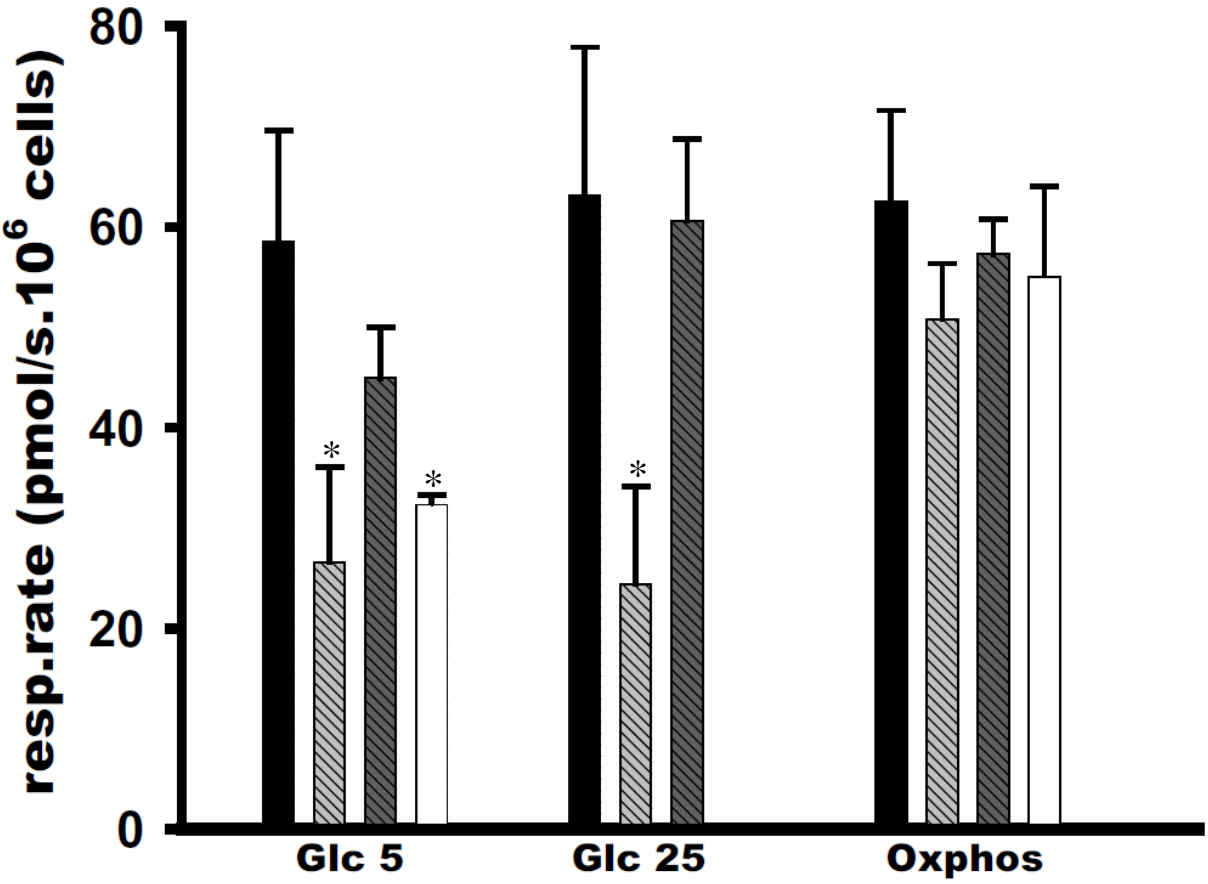

FIGURE 7 Respiratory rates of HepG2 cells in atmospheric and 5% oxygen. Cellular respiration rates, *i.e.* without any agents added, are shown for the following conditions (defined in the text): *black bars*: normal; *dashed light grey bars*: adapted; *dashed dark grey bars*: instant adapted; and *white bars*: recovered.

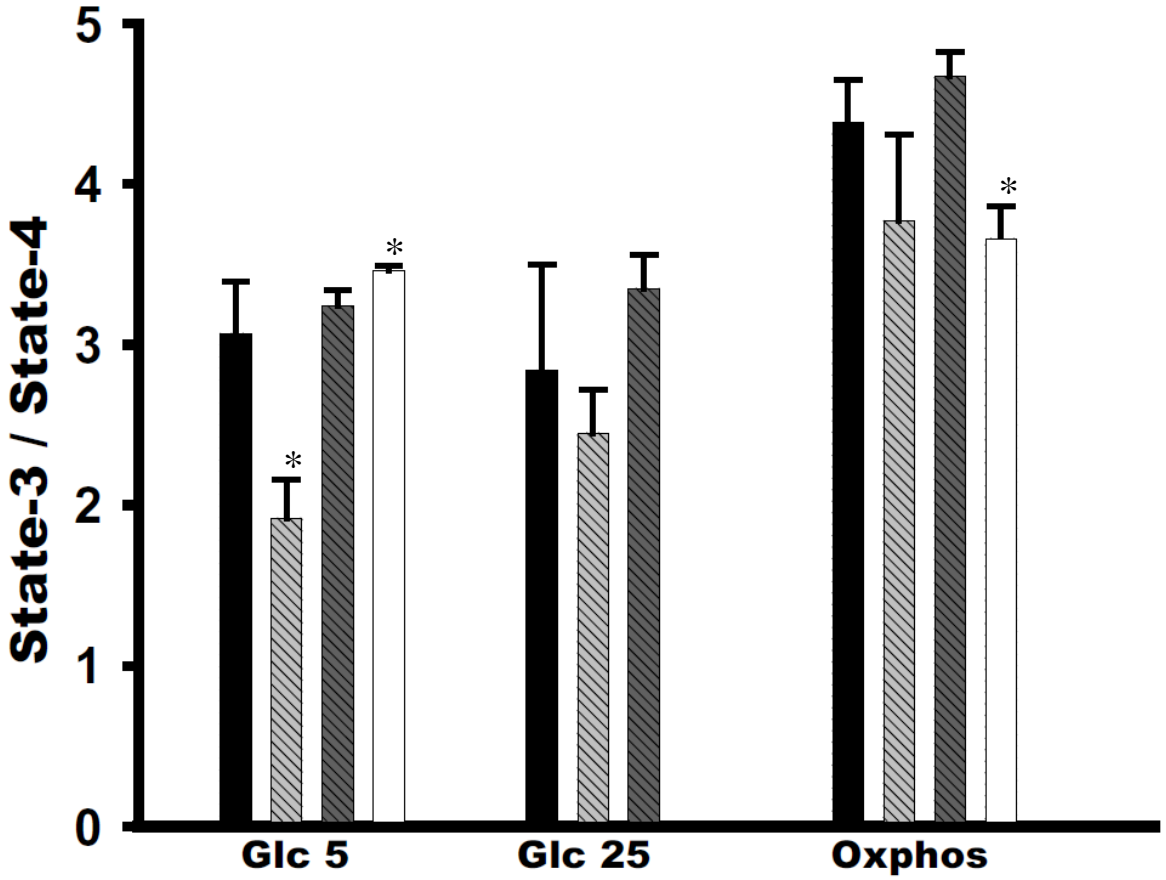

FIGURE 8 State 3/state 4 respiratory control ratios of HepG2 cells in atmospheric and 5% oxygen. State 3/state 4 respiratory control ratios are shown for the following conditions (defined in the text): *black bars*: normal; *dashed light grey bars*: adapted; *dashed dark grey bars*: instant adapted; and *white bars*: recovered.

7 DISCUSSION

7.1 Mechanism of Attenuation of Mitochondrial Complex I Superoxide Production by Uncoupling

I have revealed for the first time that EIPA is a true inhibitor of H^+-pumping specific for mitochondrial Complex I (Figs. 1–2, *pages 9–10*). Employing EIPA as Complex I H^+-pumping inhibitor has important consequences on ascribing the role of conformational changes transducing redox energy of the electron transport to H^+-pumping.

Among all the matrix constituents, mitochondrial DNA (mtDNA) is the most susceptible element to oxidative stress [11]. When mtDNA mutations happen to occur in the coding regions of Complex I H^+-pumping subunits (*e.g.* ND5, ND2, or ND4), the consequent retardation of H^+-pumping would presumably cause increased $O_2^{\bullet-}$ production by Complex I and more pronounced oxidative stress [2, 6]. By this mechanism the continuous self-accelerating vicious cycle augments oxidative damage until an ultimate threshold for apoptosis and/or pathological condition is met [1].

We show for the first time that uncoupling is not efficient enough to attenuate Complex I-derived $O_2^{\bullet-}$ production under circumstances when H^+-pumping is disabled, *i.e.* by EIPA in the experimental set-up or by mutated Complex I subunits in diseases.

7.2 Targeting of $MitoQ_{10}$-related Therapeutics to Oxidative Stress

Excessive production of Complex I-generated $O_2^{\bullet -}$ can be alleviated by mild uncoupling, achieved either by artificial uncoupler or through the action of uncoupling proteins [12], or by $MitoQ_{10}$, which attenuates rotenone-induced $O_2^{\bullet -}$ production by accelerating electron flow within Complex I (Fig. 4, *page 13*) [3]. The main advantage of $MitoQ_{10}$ over uncoupler-based antioxidants is that it remains effective even when H^+-pumping by Complex I is hindered, as is the case of aging and diseases arising from accumulation of oxidative damage to segments of mtDNA encoding Complex I H^+-pumping subunits ND2, ND4, and ND5 [2, 6]. This fact makes mitochondria-targeted antioxidants worthy candidades when considering effective therapeutic intervention.

Our hypothesis provides a considerable insight into the mechanism of $MitoQ_{10}$ action, clearly demonstrating the conditions favoring either the pro-oxidant or anti-oxidant effects of $MitoQ_{10}$, and explaining why different research groups arrived to contradictory conclusions about the possible antioxidant properties of $MitoQ_{10}$. The observation that $MitoQ_{10}$ raises $O_2^{\bullet -}$ production in intact mitochondria has important consequences on the potential use of $MitoQ_{10}$ as a therapeutic [3]. Mitochondria-targeted antioxidants, such as $MitoQ_{10}$ or SkQ1 [13], may efficiently prevent or treat oxidative stress-related ailments upon restricting their effect only to tissues from which oxidative stress emanates.

7.3 The Role of Mitochondrial Phospholipases in Concert with Uncoupling in Feedback Down-regulation of Oxidative Stress

Our results demonstrate the orchestrated action of mitochondrial phospholipase $iPLA_2$ and the uncoupling protein 2 (UCP2) in their common physiological function to downregulate reactive oxygen species formation (Figs. 5–6, *pages 15–16*).

Our work provides supporting data for a hypothetical feedback attenuation of lipoperoxidation by its products, *i.e.* hydroperoxy fatty acids (FAOOHs), which are released by Ca^{2+}-insensitive mitochondrial phospholipase A_2. This hypothesis suggests activation of UCP2 by lipoperoxidation products well upstream of the peroxidation cascade leading to 4-hydroxynonenal, which was proposed by Brand *et al.* to be the activating species [14]. Our interpretation supports the fatty acid cycling hypothesis that is based on the classification of UCP2 to the family of anion transporters [15]. However, the mechanism by which superoxide or other downstream ROS activate mitochondrial phospholipases A_2 remains unclear [16]. An indirect activation could conceivably stem from a preferential PLA_2 specificity to cleave hydroperoxy phospholipids (PLOOHs) rather than intact glycerophospholipds, unaffected by lipoperoxidation [17]. Our results demonstrate the presence of $iPLA_2$ in lung mitochondria and underscore the straightforward mechanism of $mtPLA_2$-mediated fatty acid hydroperoxides release to stimulate UCP2-dependent attenuation of

ROS [18].

7.4 Implementation of Physiological Normoxia Conditions as a Real Experimental Model

Experiments with cell cultures are routinely performed at an air atmosphere (~ 21% O_2). However, these conditions in terms of oxygen concentration are far away from what is going on at the level of tissues and organs [19], referred as physiological normoxia (~ 5% O_2 for liver). Morevoer, under certain pathological circumstances (ischemic disorders, diabetes, atherosclerosis, *etc.*) [19], when the demand for O_2 by the respiratory chain exceeds its supply, oxygen levels may temporarily drop even beyond a tissue-specific threshold level and attain the state of physiological hypoxia (< 5% O_2 for liver) [20]. We attempted to simulate these transient changes, mediated presumably by hypoxia-inducible factor [21], by transfering hepatocellular carcinoma HepG2 cells to 5% for the period of three days, and quantified basic respiratory parameters (Figs. 7–8, *pages 18–19*). The correctness of our model is supported by the fact that OXPHOS cells, with active oxidative phosphorylation machinery, adapted more efficiently to tissue normoxia than cells utilizing glycolysis as the main energy source, GLC5 and GLC25 cells (Fig. 7, *page 18*). On this basis, we may assume that similar adaptations occur during transfer from physiological normoxia to hypoxia *in vivo*. Such adaptation corresponded with highly repressed mitochondrial $O_2^{\bullet -}$ production on the background of efficient oxidative phosphorylation and ongoing dynamic changes of mitochondrial reticulum.

8 CONCLUSIONS

1) Accelerated electron flux and proton pumping within Complex I by uncoupling, which attenuates Complex I-derived superoxide production, cannot be in effect when proton pumping is blocked. In experiments, this block was simulated by EIPA, an inhibitor of H^+-pumping mediated by Complex I. Uncoupling can diminish ROS production but not the one resulting from damage of mtDNA linked to impairment of the proton-pumping pathway.

2) $MitoQ_{10}$ exerts its antioxidant action by bypassing electron block on Complex I *via* an alternative electron transfer pathway involving Complex II acting in the reverse mode. Unlike uncoupling, $MitoQ_{10}$ is able to possibly cure diseases arising from oxidative stress due to aberrant Complex I H^+-pumping subunits, *i.e.* coded by oxidatively damaged mtDNA, when targeted to the pathological tissue.

3) Oxidative stress attenuation by UCP2-dependent uncoupling is initiated upon the activation of mitochondrial phospholipase $iPLA_2$ as a feedback regulatory response to increased lipoperoxidation.

4) Cells with high oxidative phosphorylation content adapt to more efficient oxidative phosphorylation under conditions of physiological normoxia, whereas glycolytic normoglycemic cells adapt to physiological normoxia by elevated state 4 respiration.

9 REFERENCES

[1] Ježek, P., Hlavatá, L.: *Int. J. Biochem. Cell Biol.* 37, 2478–2503 (2005)

[2] Dlasková, A., Hlavatá, L., Ježek, J., Ježek, P.: *Int. J. Biochem. Cell Biol.* 40, 2098–2109 (2008) http://dx.doi.org/10.1016/j.biocel.2008.02.007

[3] Plecitá-Hlavatá, L., Ježek, J., Ježek, P.: *Int. J. Biochem. Cell Biol.* 41, 1697–1707 (2009) http://dx.doi.org/10.1016/j.biocel.2009.02.015

[4] Jabůrek, M., Miyamoto, S., Di Mascio, P., Garlid, K.D., Ježek, P.: *J. Biol. Chem.* 279, 53097–53102 (2004)

[5] Broekemeier, K.M., Iben, J.R., LeVan, E.G., Crouser, E.D., Pfeiffer, D.R.: *Biochemistry* 41, 7771–7780 (2002)

[6] Dlasková, A., Hlavatá, L., Ježek, P.: *Int. J. Biochem. Cell Biol.* 40, 1792–1805 (2008)

[7] Hotta, Y., Ishikawa, N., Ohashi, N., Matsui, K.: *Mol. Cell. Biochem.* 219, 83–90 (2001)

[8] Martín, C., Martínez, R., Navarro, R., Ruiz-Sanz, J.I., Lacort, M., Ruiz-Larrea, M.B.: *Biochem. Pharmacol.* 62, 705–712 (2001)

[9] Farooqui, A.A., Litsky, M.L., Farooqui, T., Horrocks, L.A.: *Brain Res. Bull.* 49, 139–153 (1999)

[10] Jekabsons, M.B., Echtay, K.S., Brand, M.D.: *Biochem. J.* 366, 565–571 (2002)

[11] Bourges, I., Ramus, C., Mousson de Camaret, B., Beugnot, R., Remacle, C., Cardol, P., Hofhaus, G., Issartel, J.P.: *Biochem. J.* 383, 491–499 (2004)

[12] Sullivan, P.G., Springer, J.E., Hall, E.D., Scheff, S.W.: *J. Bioenerg. Biomembr.* 36, 353–356 (2004)

[13] Antonenko, Y.N., Roginsky, V.A., Pashkovskaya, A.A., Rokitskaya, T.I., Kotova, E.A., Zaspa, A.A., Chernyak, B.V., Skulachev, V.P.: *J. Membr. Biol.* 222, 141–149 (2008)

[14] Echtay, K.S., Esteves, T.C., Pakay, J.L., Jekabsons, M.B., Lambert, A.J., Portero-Otín, M., Pamplona, R., Vidal-Puig, A.J., Wang, S., Roebuck, S.J., Brand, M.D.: *EMBO J.* 22, 4103–4110 (2003)

[15] Ježek, P., Ježek, J.: *FEBS Lett.* 534, 15–25 (2003) http://dx.doi.org/10.1016/S0014-5793(02)03779-1

[16] Guidarelli, A., Cantoni, O.: *Biochem. J.* 366, 307–314 (2002)

[17] van Kuijk, F.J.G.M, Sevanian, A., Handelman, G.J., Dratz E.A.: *Trends Biochem. Sci.* 12, 31–34 (1987)

[18] Mattiasson, G., Sullivan, P.G.: *Antioxid. Redox Signal.* 8, 1–38 (2006)

[19] Brahimi-Horn, M., Pouysségur, J.: *FEBS Lett.* 581, 3582–3591 (2007)

[20] Jiang, B.H., Semenza, G.L., Bauer, C., Marti, H.H.: *Am. J. Physiol.* 271, C1172–C1180 (1996)

[21] Taylor, C.T.: *Biochem. J.* 409, 19–26 (2008)

10 LIST OF AUTHOR'S PUBLICATIONS

Plecitá-Hlavatá, L., Ježek, J., Ježek, P.: Pro-oxidant mitochondrial matrix-targeted ubiquinone $MitoQ_{10}$ acts as anti-oxidant at retarded electron transport or proton pumping within Complex I.
Int. J. Biochem. Cell Biol. 41, 1697–1707 (2009)
http://dx.doi.org/10.1016/j.biocel.2009.02.015 **IF** (2007) **= 4.009**

Dlasková, A., Hlavatá, L., Ježek, J., Ježek, P.: Mitochondrial Complex I superoxide production is attenuated by uncoupling.
Int. J. Biochem. Cell Biol. 40, 2098–2109 (2008)
http://dx.doi.org/10.1016/j.biocel.2008.02.007 **IF** (2007) **= 4.009**

Raju, N., Špaček, T., Ježek, J., Caminiti, I.M., Leinisch, F., Hideg, K., Ježek, P., Trommer, W.E.: Fatty acid binding site of mitochondrial uncoupling protein UCP2 as probed by EPR spectroscopy of spin-labeled fatty acids.
Appl. Magn. Reson. 30, 373–383 (2006) **IF = 0.692**

Ježek, P., Ježek, J.: Sequence anatomy of mitochondrial anion carriers.
FEBS Lett. 534, 15–25 (2003) http://dx.doi.org/10.1016/S0014-5793(02)03779-1 **IF = 3.609**

Total IF = 12.319